Elevational patterns of temperature and humidity in the middle Tianshan Mountain area in Central Asia

Gheyur GHEYRET[1#] https://orcid.org/0000-0003-4707-8713; e-mail: gheyur@pku.edu.cn

Anwar MOHAMMAT[2#] https://orcid.org/0000-0003-4437-877X; e-mail: anwar@ms.xjb.ac.cn

TANG Zhi-yao[1*] https://orcid.org/0000-0003-0154-6403; e-mail: zytang@urban.pku.edu.cn

*Corresponding author

#Authors contributed equally

1 Institute of Ecology, College of Urban and Environmental Sciences and Key Laboratory for Earth Surface Processes, Peking University, Beijing 100871, China

2 Key Laboratory of Biogeography and Bioresources in Arid Land, Xinjiang Institute of Ecology and Geography, Chinese Academy of Sciences, Urumqi 830011 China

Citation: Gheyret G, Mohammat A, Tang ZY (2020) Elevational patterns of temperature and humidity in the middle Tianshan Mountain area in Central Asia. Journal of Mountain Science 17(2). https://doi.org/10.1007/s11629-019-5481-0

Abstract: The vertical distribution of vegetation types along an elevational gradient in mountain areas largely depends on the elevational changes in air temperature and humidity. In this study, we presented the seasonal and diurnal variations in the elevational gradients of air temperature and humidity on the southern and northern slopes in the middle Tianshan Mountain Range using data collected throughout the year via HOBO data loggers. The measurements were conducted at 12 different elevations from 1548 to 3277 m from September 2004 to August 2005. The results showed that the annual mean air temperature decreased along the elevational gradients with temperature lapse rates of (0.71±0.20)°C/100 m and (0.59±0.05)°C/100 m on the northern and southern slopes, respectively. The annual mean absolute humidity significantly decreased with increasing elevation on the northern slope but showed no significant trend on the southern slope. The annual mean relative humidity did not show a significant trend on the northern slope but increased with increasing elevation on the southern slope. The mean air temperature lapse rate exhibited significant seasonal variation, which is steeper in summer and shallower in winter, and this value varied between 0.37°C/100 m and 0.75°C/100 m on the southern slope and between 0.30°C/100 m and 1.02°C/100 m on the northern slope. The mean absolute and relative humidity also exhibited significant seasonal variations on both slopes, with the maximum occurring in summer and the minimum occurring in winter or spring. The monthly diurnal range of air temperature on both slopes was higher in spring than in winter. The annual range of air temperature on the southern slope was higher than that on the northern slope. Our results suggest that significant spatiotemporal variations in humidity and temperature lapse rate are useful when analyzing the relationships between species range sizes and climate in mountain areas.

Keywords: Temperature lapse rate; Absolute humidity; Relative humidity; Annual range of temperature; Diurnal range of temperature; HOBO data loggers

Introduction

Mountains cover approximately one-fifth of Earth's land surface, and support one- quarter of

terrestrial biodiversity, with nearly half of the global biodiversity hotspots located in mountains (Körner 2004). Mountains play important roles in shaping the regional climate through their orographic barrier effect (Beniston 2006), which is responsible for the spatial changes in climatic variables, such as rainfall, air humidity, air movement, air temperature, and solar radiation (Barry 2008). Accurate measurements of climatic elements, especially the surface air temperature and its spatiotemporal variations in the mountainous area are vital for better understanding the impacts of climate change on organisms, biodiversity and hydrological processes (Whittaker et al. 2001; Pepin et al. 2015). For example, Wason et al. (2017) investigated the climate-vegetation relationship along an elevational gradient using temperature records form data loggers and climatic stations and found that elevational distribution of spruce-fir forests was strongly correlated with summer and fall monthly temperature on mountains in the northeastern U.S. Chan et al. (2016) reported that the diurnal variations in air temperature were negatively correlated with the size of the elevational range of terrestrial vertebrates throughout the world, whereas the seasonal variations were positively correlated with the elevational range. Based on in-situ measurements of the microclimate, Tang and Fang (2006) found that the mean air temperature of the growing season (MTGS) could explain the elevational differences in timberline better than other thermal indices, such as mean temperature of the warmest month (MTWM), growing season length or warmth index (WI), on the southern and northern slopes of Mt. Taibai in Central China. These results highlight the importance of high spatial and temporal resolution measurements of climate variables when studying the distribution and performance of organisms. However, in mountainous areas, the variability in air temperature is complicated and generally regulated by various non-linear processes; this variability is affected by large-scale atmospheric circulation characteristics, local-scale air flows, interactions between topography and air-flow, solar radiation and other ground surface features, such as soil and vegetation types (Barry 2008). Moreover, mountain ecosystems are exceptionally fragile and sensitive to global warming (Körner 2004) and are experiencing more rapid climate change than other areas (Wang et al. 2013; Deng et al. 2015; Pepin et al. 2015). However, the estimation of climate change in mountains presents a major challenge to scientific communities and local managers, as climatic stations are very sparse in mountain areas. The challenge is more critical at mid- and high-elevations in remote areas and over complex terrain, where climatic stations are usually sparse or unavailable mainly because of the inconvenience of installing and maintaining climatological stations (Chae et al. 2012).

The temperature lapse rate (TLR) commonly used to extrapolate air temperature from point measurements to sites at different elevations where measurements are scarce. Traditionally, a constant adiabatic TLR in the range 0.60°C/100 m to 0.65°C /100 m has been used in gridded analyses (Prentice et al. 1992; Ngo-Duc et al. 2005); however, this value could be inappropriate because it neglects the topographical features and other local factors (Minder et al. 2010; Shuttleworth 2012; Kirchner et al. 2013). Other approaches, such as station-based spatially interpolated and satellite remote sensing datasets, have also been employed to obtain the local climate conditions in mountain areas (Li et al. 2013; Zhang et al. 2018). Interpolating point records to the gridded data at regional or global scales would not accurately represent the natural variability in temperature along the elevational range in mountainous areas due to the low spatiotemporal resolution (Li et al. 2013; Minder et al. 2010).

Near the surface, temperature generally decreases with increasing elevation, and the TLR is usually negative (Fang and Yoda 1988); however, the TLR can be positive when the inversion effect, cold air drainage or the foehn effect occur (Blandford et al. 2008). For example, during the cloud-free nights in colder months, the calm higher-pressure events result in the descent of cold, dense air along the slopes down to the bottom of the valley, producing an inversion layer, i.e., the air in the mountain valley that is colder than the air above that layer (Lundquist et al. 2008; Pagès et al. 2017). This cold air at the surface fills in the topographic depression confined by the nearby higher terrain and becomes stagnant, which is a process called cold air pooling (Lundquist et al.

2008). Therefore, some previous studies reported obvious spatial and temporal variations in the TLR in mountain regions (Lundquist et al. 2007; Li et al. 2015). A significant change in the TLR at both diurnal and seasonal time scales was caused by the variation in sensible heat flux between the free air and the near-surface air. Pepin (1994) and Rolland (2003) found that the TLR was steeper in spring/summer than in winter and steeper during the daytime than at night. The steeper TLR in warmer months could be attributed to the increase in solar radiation, which increases the near-surface air temperature, whereas the shallower TLR in winter was a consequence of the monsoon airflow induced the inversion effect (Blandford et al. 2008; Li et al. 2015). Additionally, the variation in free air instability and terrain conditions also affected the seasonal variations in the TLR (Barry 2008; Li et al. 2015). Diurnal changes in the TLR correspond to the variation in synoptic weather conditions (Gardner et al. 2009). During the day, increases in surface air temperature at lower elevations were more rapid than those at higher elevations under the same radiation conditions, and this asymmetric effect resulted in the TLR being steeper during the daytime than during the night (Barry 2008). At night, the increased frequency of the inversion effect mentioned above would contribute to the diurnal change in the TLR. However, the spatial variability in the TLR usually depends on topographic features and synoptic weather types. In a previous study, Li et al. (2013) investigated the spatial changes in the TLR in mainland China using records from 533 climatic stations and found that the TLR exhibited a banded distribution from northwest to southeast and that the values on the Tibetan Plateau were steeper than those in other parts of China, which corresponded to the variations in air temperature, relative humidity and topography. Thus it is not appropriate to use the fixed lapse rate to interpolate the temperature.

The lack of climatic stations is more severe in Central Asia, where most of the climatic stations stopped working after the fall of the Soviet Union in 1991 (Schiemann et al. 2008), and the stations that currently work are unevenly distributed or rare in high-elevation regions, where ecological researches hihgly focus. As a result, little information is provided about the spatial or temporal (i.e., interannual-, seasonal- and diurnal-scale) variation in the air temperature and humidity in this region. For this reason, more accurate and real climatic data along the full elevational range are required to reveal the actual relationships between climate and vegetation distribution.

The Tianshan Mountain Range, which is located in the centre of the Eurasian Continent, is characterized by a large elevation range, from 154 m below sea level to 7439 m above sea level, which results in significant changes in air temperature, precipitation and soil properties and thus displays clear vertical patterns of vegetation types and diversities. In addition, the Tianshan Mountain Range is regarded as the "water tower" of Central Asia, because the high snow cover and glacier extent at the top of the mountains (i.e., 3800-5000 m a.s.l.) are the main water resources for the oasis and desert ecosystem in Central Asia; however, this area is highly susceptible to climate change (Sang 2009). Therefore, accurate measurements of the spatial variations in climatic variables are crucial for understanding the hydrological processes in this region (Minder et al. 2010).

In this study, we present the results of a full year of climatic measurements over an elevational range of 1500 m on both the southern and northern slopes of the middle Tianshan Mountain area. Although the fieldwork is not recent and the collected data was old, our study can still provide basic information for future research on the vegetation-climate relationship because the Tianshan Mountains show a significant vertical distribution of vegetation. The objective of this paper is to investigate the elevational and seasonal patterns in humidity and air temperature and the potential causes of their variations over different slopes in arid regions.

1   Materials and Methods

1.1 Study area

The Tianshan Mountain Range (39°30´– 45°45´N, 74°10´–96°15´E) is the largest mountain system located in arid Central Asia and stretches 2500 km from west to east, with peaks ranging from 4000-6000 m (Sobel et al. 2006; Zhang et al. 2018). In China, this mountain range is located

between the vast Tarim Basin to the south and the Junggar Basin to the north in the Xinjiang Uyghur Autonomous Region (Guo and Li 2015). Far from the Oceans, the region demonstrates typical continental climate characteristics with relatively warm and humid summers, cold and dry winters and large diurnal air temperature range (Xu et al. 2018). Tianshan Mountain Range constitutes a physical barrier that intercepts the northern and western air masses from Siberia and Kazakh grasslands, so that they cannot reach Central Asia, ultimately causing a drought-dominant climatic patterns and life zones in that region. The effect of Tianshan Mountain Range on Central Asia is similar to that of the Himalayas on their North (Aizen et al. 1997). According to the Urumqi-Mushi climate station on the northern slope (87°07´ E, 43°16´N, 2350 m) and the Baluntai climate station on the southern slope (86°07´E, 42°66´N, 1752 m), the annual mean precipitation is 511 mm and 214 mm, and the temperature is 2.9°C and 7.6°C, respectively (Figure 1). Recent studies showed that 7934 glaciers were distributed in the China parts of the Tianshan Mountain Range, with total areas and volumes of 7179.77 km² and 707.95 km³, respectively (Liu et al. 2015), and these glaciers are
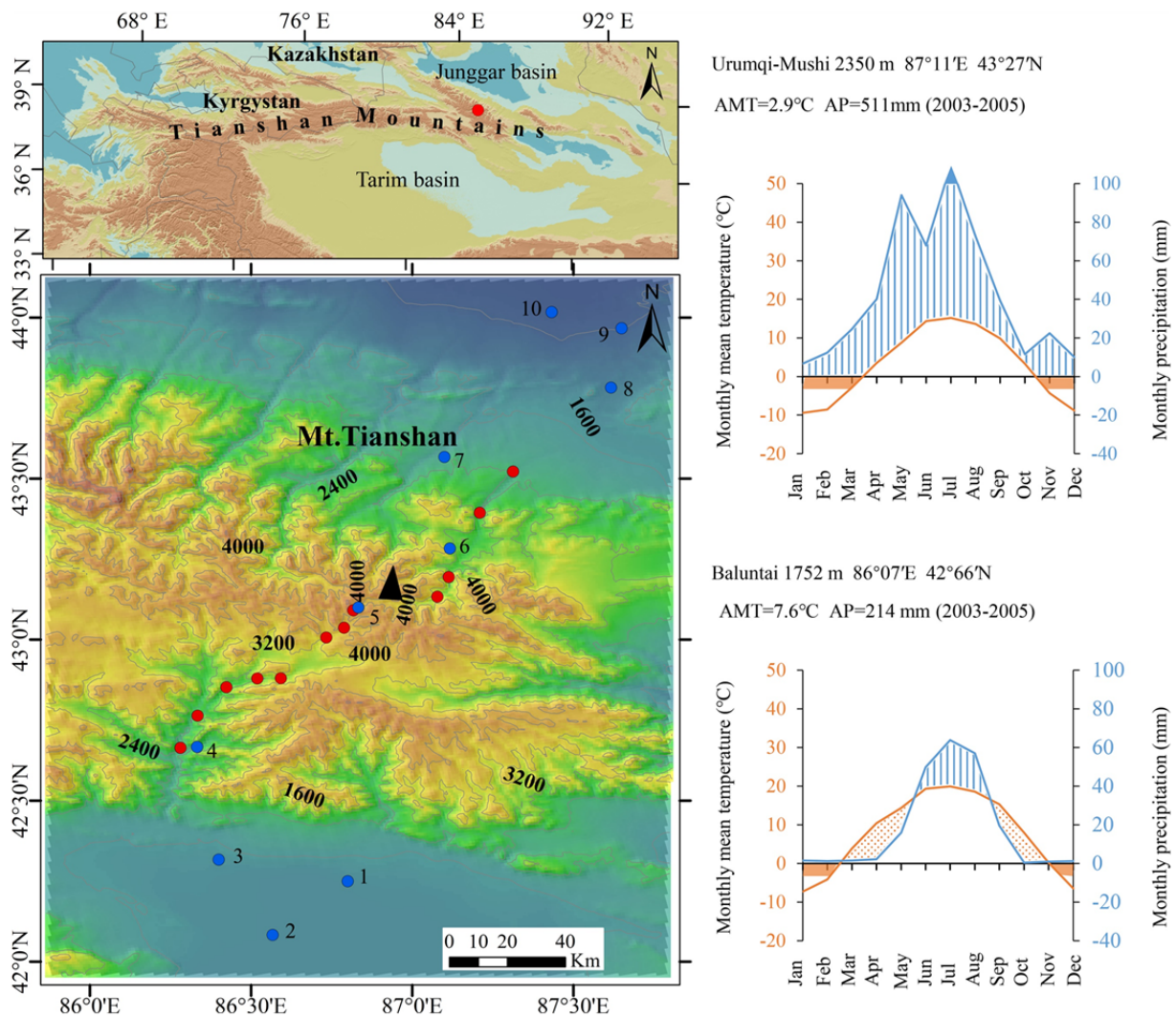

Figure 1 Distribution of observation sites along the southern and northern slopes in the Tianshan Mountain Range. The contour interval on the topographic map is 800 m. The upper left subset shows the location of the study area in Central Asia, and the right subset shows the climate characteristics of nearby stations on the northern (Urumqi-Mushi) and southern slopes (Baluntai). AMT: annual mean temperature; AP: annual mean precipitation. Red dots and blue dots in the lower-left subset represent the locations of data loggers and climatic stations, respectively. The Numbers corresponding to the blue dots refer to the names of the 10 climatic stations used in the present study: 1. Heshuo, 2.Yanqi, 3. Hejing, 4. Baluntai, 5. Daxigou, 6. Urumqi-Mushi, 7. Xiaoquzi, 8. Urumqi, 9. Miquan, 10. Changji.

vital for the sustainability of the oases and desert areas in this region.

The vegetation structure exhibits an obvious vertical distribution in the mountains. Along the northern slope, the vegetation changes from desert (below 800 m with dominated by *Artemisia rupestris*), desert steppes [800, 1100) m with *Artemisia* sp.), forest-steppe ecotone [1100, 1720) m with *Stipa glareosa* and tree species of *Picea schrenkiana and Salix* sp.), Tianshan *spruce* forest [1700, 2800) m, with *Picea schrenkiana*), alpine and subalpine meadow [2800, 3400) m with *Polygonum viviparum*) and alpine cushion vegetation [3400, 3900) m with *Thylacospermum caespitosum*) to glacier and perennial snow cover ⩾ 3900 m (Sang 2009; Pan et al. 2013). On the southern slope, the vegetation changes from desert (below 1800 m dominated by *Anabasis* sp.), mountain steppes [1800, 2200) m with *Artemisia macrocephala*), subalpine forest-steppes [2200, 3000) m with *Stipa capillata* sp. and tree species of *Picea schrenkiana*) and alpine meadow [3000, 3600) m with *Festuca ovina*) to glacier and snow cover ⩾ 3600 m (Liu 2017).

1.2 Measurement of temperature and humidity

To explore the spatial changes in air temperature, 15 electronic HOBO H8 data loggers (Onset Computer Corporation, Cape Cod, MA, USA; a temperature sensor with a measuring range from -30°C to +50°C , accuracy of ±0.2°C) were installed at a height of 0.5 m above the ground along the northern slope between 1548 m and 2826 m and along the southern slope between 1569 m and 3598 m at an interval of approximately 300 m in the study area (Figure 1), and Table 1 provides the characteristics of each location. The measurement of the elevation at each location was implemented with a Barigo altimeter. To ensure the accuracy of the data and sensor stability (deviation from zero ±0.2 ℃), the loggers were tested in an ice-water bath before and after exposure. The data loggers in our study were placed in cylindrical plastic pipes with open ends to protect from direct radiation and to allow adequate ventilation. Because there were no trees at most of our measurement sites, we attached and tied the plastic pipes to the shrub canopies horizontally, with the pipes facing from north to south. Because the height of the shrubs at our sites was mostly approximately 0.5 m, to ensure the same installation height at all sites, we attached the data loggers 0.5 m above the ground. The measurements of air temperature and humidity began at 00:00 on July 1, 2004, and stopped at 21:00 on September 27, 2005. The interval was set to 0.5 h, and the local solar time, i.e. Coordinated Universal Time (UTC) + 6 was used in the present study. Considering that there were large fluctuations in the data in July and August of 2004 that differed from our normal dataset, we believe this period represents an adaptation time for sensor; for this reason, we did not use the data from this period in this study. Thus, only the data recorded from 00:00 on September 1, 2004 to 23:30 on August 31, 2005 were used in this study, and no corrections were made. At the end of the measurement period, we found that the data loggers at the sites at 2680 and 3598 m a.s.l. on the southern slope and site at the site 2598 m a.s.l. on the northern slope were broken into pieces; thus, we obtained 12 observations over a one-year period of air

Table 1 Characteristics and description of the different locations where the 12 data loggers were installed.

Location	Lat.(°N)	Long.(°E)	Ele.(m)	Aspect	Slope	Topography	Vegetation type
Northern slope	43.5220	87.3128	1548	NE	7.06°	Valley floor	Desert scrub
	43.3936	87.2096	1997	NE	19.07°	Valley	Forest-steppe ecotone
	43.1942	87.1135	2152	NE	9.64°	Valley	Mountain shrubby steppe
	43.1330	87.0782	2402	NE	10.62°	Valley	Spruce forest
	43.0910	86.8173	2826	NE	7.86°	Slope	Alpine shrubby meadow
Southern slope	42.6637	86.2812	1569	SW	8.77°	Valley	Desert scrub
	42.7637	86.3341	1741	SE	6.64°	Valley	Desert scrub
	42.8522	86.4238	1990	SE	7.37°	Valley	Mountain shrubby steppe
	42.8795	86.5193	2222	SE	3.13°	Valley	Mountain shrubby steppe
	42.8799	86.5924	2414	SE	3.68°	Valley	Subalpine forest-steppe
	43.0067	86.7333	2990	SE	7.40°	Slope	Subalpine forest-steppe
	43.0368	86.7884	3277	SE	14.54°	Slope	Alpine shrubby meadow

temperature and humidity data. The elevational range of the data loggers was relatively small given the entire range of the Tianshan Mountains. However, it is difficult to reach the mountain-top to install data loggers at the upper altitudes (>3900 m) of the middle Tianshan Mountain area where glacier and snow covered (Sang 2009; Pan et al. 2013).

1.3 Data analysis

To understand if the data collected through data loggers represent the long-term climatic pattern in our study area, we compared the actual data from the data loggers with that interpolated from observation stations. For this reason, we applied multiple regression and explored the relationship between air temperature (obtained from both climatic stations and data loggers) and latitude, longitude and elevation using the following model, which is commonly used to interpolate local climate conditions (Fang and Yoda 1988):

$$AMT = a_0 + a_1 \times Lat + a_2 \times Long + a_3 \times ELE \quad (3)$$

where a_1, a_2 and a_3 are regression coefficients, and a_3 is also the elevational TLR of temperature. Then based on this relationship, we calculated the extrapolated the AMT (annual mean temperature) for each observation site in our study. We used monthly air temperature records during the periods of 2003-2005 from 10 climatic stations (6 on the northern slope and 4 on the southern slope) near the study area (Figure 1) within a latitudinal range of 42°04´- 44°01´N, and a longitudinal range of 86°19´- 87°39´E.

Four humidity indices, i.e., monthly mean absolute (MMAH) and relative humidity (MMRH) and annual mean absolute (AMAH) and relative humidity (AMRH), and five temperature indices, i.e., monthly mean temperature (MMT) and AMT, monthly (MDRT) and annual mean diurnal range of temperature (ADRT), and annual range of temperature (ART), were computed to investigate the elevational and temporal changes in humidity and air temperature. The MMRH, MMAH and MMT were averaged arithmetically according to the daily mean values of (average values of 48 records per day, and one record per 0.5 h) relative and absolute humidity and temperature in each

month. The AMRH, AMAH and AMT were an averaged arithmetically from 12 MMRH, MMAH and MMT values. The MDRT was the mean values of the diurnal range of temperatures (DRT) (difference between the daily maximum and minimum temperatures) in each month, and the ADRT was the mean value of 12 MDRT values. The ART was the difference between the MMTs of the warmest and coldest months. To investigate the diurnal change in the TLR, we calculated the average hourly air temperature at each site (2 records per hour and 48 records per day) for different dates throughout the year, which was important for exploring the climatic pattern (Fang and Yoda 1988; Tang and Fang 2006). Linear regression was used in this study to investigate the elevational patterns of these climatic indices. The TLR was represented by the coefficient calculated through an ordinary least squares regression line that was fitted to temperature against elevation (Rolland, 2003; Minder et al., 2010).

2 Results

2.1 Comparison of temperature from the data loggers versus climatic station

Comparing data from the data loggers and those interpolated from observation stations showed that at most elevations, both data fit well, except for the much lower values at 2826 m on the northern slope using mean daily temperature (Figure 2a), suggesting that the climate pattern in the Tianshan Mountain Range is well represented by data from data loggers. We also made a similar comparison using mean daily maximum (Figure 2b) and minimum (Figure 2c) temperatures separately. The results showed that extrapolated values were lower than observations for mean daily maximum temperature, but for mean daily minimum temperatures, extrapolated values were higher than observations. This may be caused by climate variation, local topography, soil type, etc.

2.2 Elevational variations in temperature and humidity

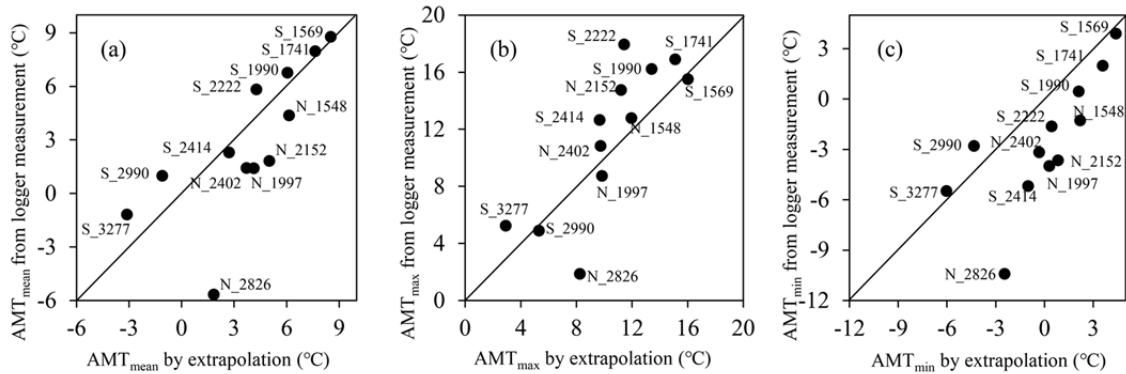On both slopes, the AMT decreased with increasing elevation, and the TLR on the northern

Figure 2 Comparison between the AMT_{mean} (a), AMT_{max} (b) and AMT_{min} (c) measured by loggers and that extrapolated using multiple regression against long-term observations. Elevation of each data-logger site is given.
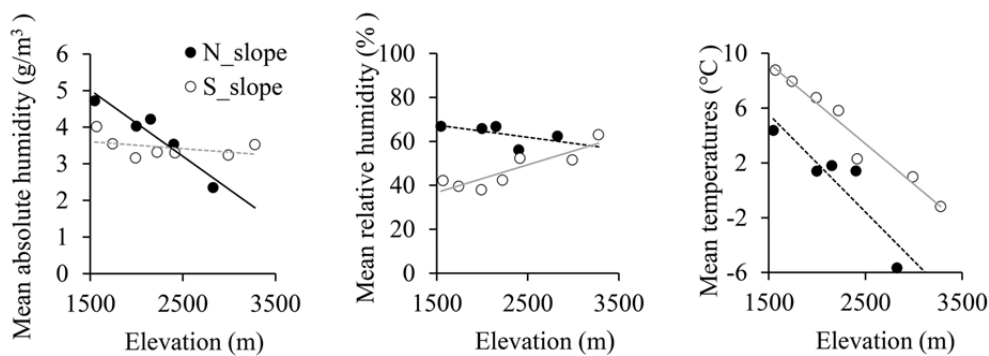

Figure 3 Elevational variations in annual mean air humidity (AMAH, g/m³), relative humidity (AMRH, %) and temperature (AMT, °C) along the southern and northern slopes of the Tianshan Mountain Range.

slope was steeper than that on the southern slope (Figure 3).

The mean AMAH was 3.8 g/m³ on the northern slope and 3.4 g/m³ on the southern slope. The AMAH showed decreasing trends from low to high elevations on the northern slope but did not show any significant trend along the southern slope (Figure 3). The mean AMRH on the northern slope was higher than that on the southern slope. The AMRH did not show any trend with elevation along the northern slope but showed an increasing trend with increasing elevation on the southern slope (Figure 3).

2.3 Seasonal changes in temperature and humidity

The maximum MMT value occurred in July, while the minimum occurred in January on both slopes. In July, the MMT decreased with increasing elevation on both slopes. In January, along the northern slope, the MMT varied from -17.6°C (at 2826 m) to -12.6°C (at 2402 m) and from -14.7°C (at 2414 m) to -7.8°C (at 1569 m) along the

southern slope (Figure 4a, 4b).

On both slopes, the MMAH showed unimodal curves, with maximum values appearing in summer, and minimum values appearing in winter (Figure 5a, 5b). The MMRH also varied seasonally, with the highest value in August and the lowest value in April for both slopes, and the MMRH on the southern slope was smaller than that on the northern slope, on average (Figure 5c, 5d).

2.4 Diurnal changes in absolute and relative humidity

Mean absolute humidity significantly decreased from low to high elevation at each time point before 10:00 a.m. Then, the elevational trend weakened at 2152 m (sudden increase), but the overall trend showed a significant decrease on the northern slope; on the southern slope, it decreased significantly from 1569 to 1990 m until it plateaued (or slightly increased) from 1990 to 2414 m (or 2990); then it dropped to the lowest value at 3277 m; however, the overall trend also showed a significant decrease (Figure 6a, 6b). The highest

value of the daily absolute humidity for the southern slope appeared at midnight, and the lowest value appeared in the afternoon, except for the patterns at elevations of 2990 and 3277 m; however, on the northern slope, there were different trends at different sites. For the mean relative humidity, the elevational trends were not significant at most time points on the northern slope; on the southern slope, they did not show a significant trend from 1569 to 2222 m and then increased to the maximum at 3277 m. In general, the highest mean relative humidity values were observed in the morning, and the lowest values were observed in the afternoon on both slopes
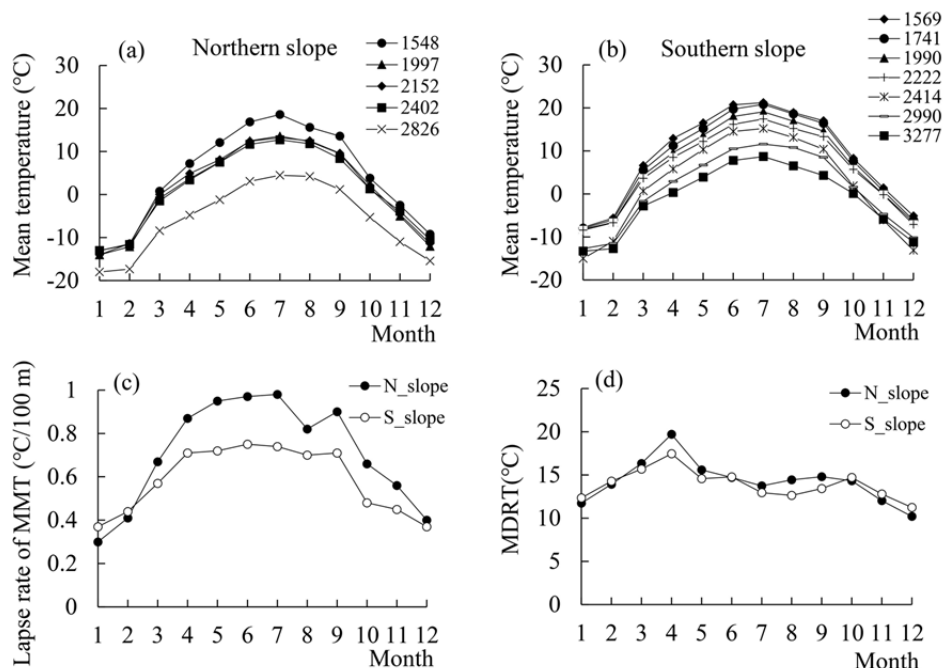

Figure 4 Monthly mean temperature (MMT) (a, b), lapse rate of temperature (c) and monthly mean diurnal range of temperature (MDRT) (d) for each site on the northern and southern slopes of the Tianshan Mountains.
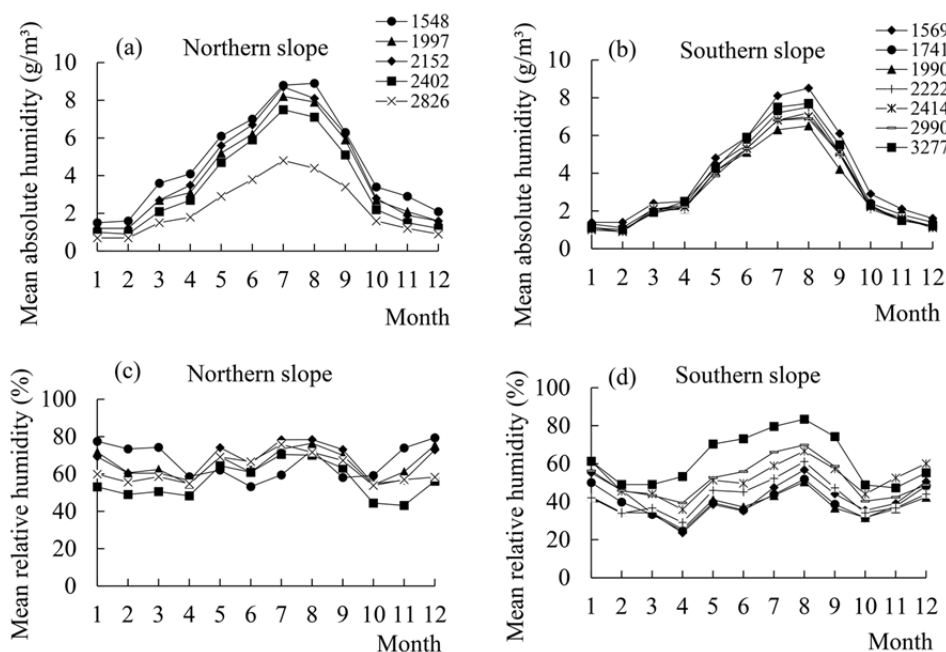

Figure 5 Monthly mean absolute and relative humidity for each site on the northern and southern slopes of the Tianshan Mountains.

(Figure 6c, 6d).

2.5 Diurnal and seasonal changes of TLR

The TLR changed significantly from 08:00 a.m. to 06:00 p.m. on the northern slope and from 10:00 a.m. to 02:00 p.m. on the southern slope during the day (Figure 7c). The TLRs were highest at noon and lowest in the afternoon and morning for both slopes (Figure 7c). The TLR also showed significant seasonal variation; the highest value appeared in July, and the lowest value appeared in January for both slopes (Figure 4c). On average, the TLR on the northern slope were steeper than those on the southern slope for all months.
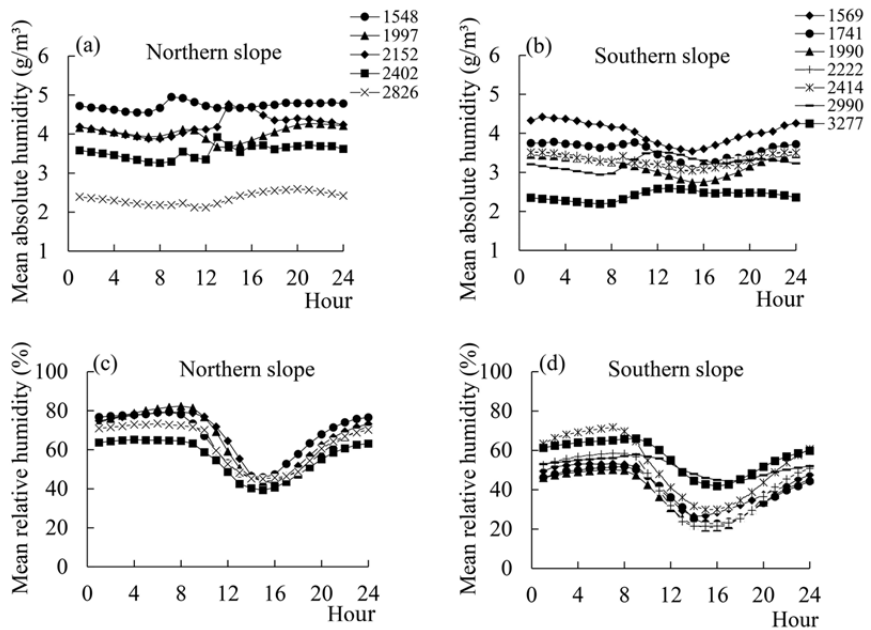

Figure 6 Diurnal variation in annual mean absolute and relative humidity along the southern and northern slopes of the Tianshan Mountain Range. The local time was used in analysis, i.e. UTC +6.

2.6 Diurnal and annual ranges of temperature

Along the elevational gradient, the ADRT did not show any significant pattern (Figure 8); it varied from 12.3°C (at 2826 m) to 18.4°C (at 2152 m) on the northern slope and from 7.7°C (at 2990 m) to 19.6°C (at 2222 m) on the southern slope. Seasonally, the highest MDRTs appeared in April, and the lowest appeared in December for both slopes (Figure 6d). The ART decreased with elevation for both slopes (Figure 8) as follows model:

$$ART_N = -0.0072H + 42.5 \ (R^2 = 0.99) \qquad (1)$$

$$ART_S = -0.0037H + 35.4 \ (R^2 = 0.68) \qquad (2)$$

where ART_N and ART_S are the annual ranges of temperature for the northern and southern slopes, respectively, H is the elevation in meters, and R^2 is the goodness of fit of the linear regression model.

3 Discussion

3.1 Validation of temperature from the data loggers

There are several possible explanations for the observations that are lower than the extrapolated values for mean daily temperature. First, local-and regional- processes, such as the cold airflow from hilltop and slope sites or blockage of cold air masses by relief, may result in lower air temperature, which may also have effects on the local air temperature (Barry 2008; Pepin et al. 2011); second, different vegetation types (e.g. tree, shrub, grass or cushion), local topography (inclination and slopes), sunshine duration or strong wind shear may result in the variation in evaporative force, which may contribute to this difference (Körner 2007). Similarly, Wang et al. (2017) found that observation values from data loggers were higher than the extrapolated values on the northern slope of the western Qinling Mountain range, partly because of the mass elevation effect. Our results also suggest that extrapolating the climate of the mountain tops from climatic stations at lower elevations (i.e., elevations of ≤ 2000 m a.s.l.) may overestimate the temperature (Duane et al. 2008); thus, we need to be cautious when using data from low elevations to estimate the climate of high mountain areas. For mean daily maximum temperature most of sites are varied around the line, but for the minimum temperature, sites mostly below the line, this may
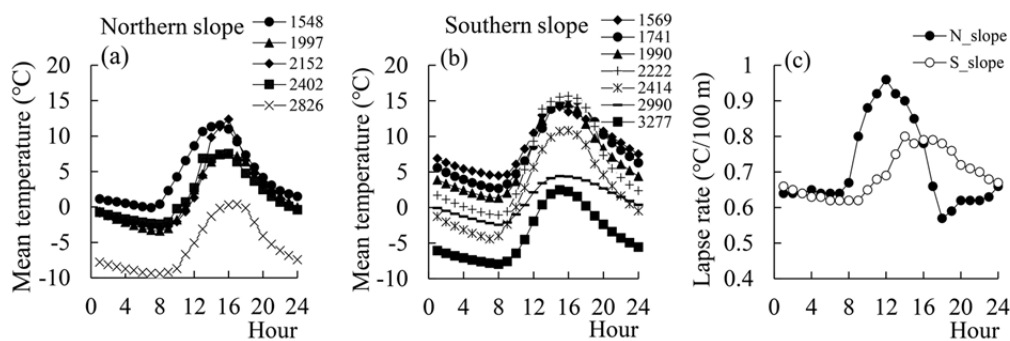
Figure 7 Diurnal variation in annual mean temperature (a, b) and lapse rates (c) along the southern and northern slopes. The hourly lapse rate was an average lapse rate of the same time for different dates between 1 September 2004 and 31 August 2005. The time zone UTC +6 was used in analysis.

suggests that there is cold air drainage at some of these logger locations.

3.2 Temperature comparisons between the northern and southern slopes

The southern slope (leeward slope) of the Tianshan Mountain Range is drier than northern slope (windward slope) (Guo and Li 2015; Shen et al. 2018). Because water vapor is largely transported from west and north of the area, precipitation occurs as the airflow rises along the windward slope, while the air that crosses over to the leeward side of the mountain is mainly dry (Beniston 2006). This phenomenon has been confirmed in the present study, which showed that the mean absolute humidity was higher at the northern slope sites than at the southern slope sites (3.8 g/m3 *vs.* 3.4 g/m3).

The TLR determines the stability of the air mass and hence plays an important role in climate formation in mountain areas and varies with the local topography, direction of airflow, latitude, solar radiation input and distance from the nearest coast (Blandford et al. 2008; Shuttleworth 2012; Kirchner et al. 2013). It is commonly acknowledged that the TLR is shallower in moist or cooler environments and steeper in drier or warmer environments because of the increased solar radiation input (Blandford et al. 2008; Gardner et al. 2009; Minder et al. 2010).Indeed, we found a steeper TLR for the Tianshan Mountain Range (0.59°C/100 m for the southern slope and 0.71°C/100 m for the northern slope) than that from a humid mountain range, Mt. Taibai (0.34°C/100 m for the northern slope and 0.50°C/100 m for the southern slope) in central

China (Tang and Fang 2006). This difference was observed because the Tianshan Mountain Range is more distant from the ocean and drier than Mt. Taibai. Similarly, Chen et al. (2018) found that the TLR of air temperature for Sygera Mountain on the southeast Tibetan Plateau was 0.50°C/100 m, and was shallower than that for Tianshan Mountain, probably because Sygera Mountain is wetter than the Tianshan Mountain areas.

Meanwhile, on both slopes, we observed a steeper the TLR in summer than in winter, due to the strong solar radiation input and maximum dry convection in summer, as well as the temperature inversion in winter (Rolland 2003; Kirchner et al. 2013; Li et al. 2015). Additionally, consistent with several previous studies, the TLR was high at noon or afternoon and low at night or in the morning (Tang and Fang 2006; Minder et al. 2010; Petersen and Pellicciotti 2011), partly because of the asymmetric effect of solar radiation at different elevations and nighttime temperature inversion (Li et al. 2015). However, when comparing the different slopes within the mountain, we found that the TLR on the southern slope (although drier) was not steeper than that on the northern slope, possibly because the cold air pooling at low elevations and more exposure to warm airflow at higher elevations resulted in decrease in the TLR and the formation of a temperature inversion on the leeward slope (Rolland 2003; Pagès et al. 2017). In prior studies, Li et al. (2013) and Shen et al. (2016) reported that temperature inversions in the winter months are a common phenomenon in the Tianshan Mountains, which would weaken the temperature-elevation relationships. They also noted that local topography (i.e., mountain valley) could also influence the atmospheric structure.

During the cloud-free nights in winter, the calm high-pressure events result in the descent of cold dense air along the leeward slope down to the bottom of the valley, producing the inversion layer, i.e., air in the mountain valley that is colder than the air above the layer (Lundquist et al. 2008; Pagès et al. 2017). Indeed, we found that at the altitude of 2414 m, a temperature inversion (measured by the mean difference in temperature between site 2414 m and 2990 m) mainly occurred in winter on southern slope, whereas in summer there were no inversion observed or the intensity of inversion were weak (Appendix 1). In addition, we found that stronger inversion in night-time (3.15) than that in daytime (0.77) in winter at an altitude of 2414 m on southern slop. In summer there were no inversion in day or night, even though the mean difference in temperature between site 2414 m and 2990 m lower in night-time (-0.51) than that in daytime (-6.57) (Appendix 1). From this perspective, we can conclude that site at 2414 m on the southern slope was influenced by the sharp inversion effect in nights in winter. This cold air at the surface filled in the topographic depression confined by the nearby higher terrain and became stagnant, which limited the temperature exchange between high elevations and lowlands. Our results are consistent with a study by Chen et al. (2018), who found that the TLR on the warm slope was smaller than that on the cool slope on Sygera Mountain, which was partly due to the different vegetation types on the two slopes. However, our finding is contrary to that of Tang and Fang (2006), who found that the TLR on the northern slope was steeper than that on the southern slope due to the climate on the northern slope being much drier than that on the southern slope.

3.3 Elevational patterns of humidity on northern and southern slopes

Our study showed that the annual mean absolute humidity (AMAH) decreased with elevation on the northern slope but showed no significant trend on the southern slope (Figure 3). This phenomenon might be because air expands and cools with increasing elevation; the extra water vapor is then dropped through condensation when the moisture is saturated (Pepin 1994) on the northern slope. However, on the southern slope,

the absolute humidity did not change significantly, probably because the air moisture was not saturated even when the air temperature decreased with increasing elevation. This result can be further illustrated by the higher annual mean relative humidity (AMRH) on the northern slope than on the southern slope (63.6% vs. 47.0%). In addition, higher forest shelter and grassland coverage on the northern slope may increase the extent of convective cloud systems and create cooler and wetter conditions by increasing transpiration compared with that on the southern slope. The mean relative humidity generally increased with elevation on the southern slope, probably because at lower elevations, the air was warm and the dew point and the air temperature were far apart. With decreasing air temperature, saturated vapor pressure will decrease and absolute humidity will remain constant, so the possibility of saturation will increase. On the northern slope, the relative humidity did not show a clear pattern with elevation because the humidity easily became saturated at all sites along the slope. We also found that both the absolute and relative humidity on the two slopes reached their maximum during the summer due to the abundant summer rainfall that contributed to increased air moisture, while in winter, the strong influence of the Siberian anticyclonic circulation decreased precipitation (Aizen et al. 1997).

In the present study, we measured the air temperature and humidity along the elevational gradient on both the northern and southern slopes of the Tianshan Mountains; thus far, no relevant studies have been conducted in this area. Thus, our results can be helpful to better understand the relationships between species distribution and climatic conditions and can provide basic information for future research in these areas. However, we also note the drawbacks and limitations of our approach and the dataset. First, the data were old, and they may not be applicable to analyse the current vegetation-climate relationships in this area because the elevational range of some vegetation types and the altitude of the treeline might have changed due to climate change over the past decade. Second, the study period was not long enough for us to explore the interannual variation in the TLR on both slopes. Third, the elevational range of measurements was

insufficient to extrapolate to the full elevational range of this mountain. In addition at some sites data might have been influenced by local factor, for example, the diurnal range of temperature in April at the altitude of 2152 m on the northern slope was much higher in comparison with other sites (Figure 4d, Appendix 2), this might be due to the reflected radiation from snow heated on the sensor.

4 Conclusion

In this study, we analyzed the spatial-temporal changes of air temperature and humidity along elevational the gradient on the Tianshan Mountains based on 12 HOBO data loggers at different elevational sites. The conclusions are as follows. 1) The TLR on the northern slope was steeper than that on the southern slope and exhibited a significant seasonal difference, as the values in the summer were steeper than those in the winter. 2) The monthly mean diurnal range of temperature (MDRT) showed significant seasonal variations, with values that were higher in spring than in winter for both slopes; the annual range of temperature (ART) on the southern slope was higher than that on the northern slope. 3) The maximum value of mean absolute (MMAH) and relative humidity (MMRH) were observed in

summer, whereas minimum values were observed in winter and spring on both slopes. Our results suggested that when investigating the vegetation patterns and their relationship with climates in mountain areas, the temporal and spatial patterns of the TLR should be taken into account. Although our findings may not be applicable to other mountain areas in the world, they can provide accurate data to identify the elevational-dependent hydrological and other ecological processes in this area. It provide researchers with valuable information to analyse the vegetation patterns, species elevational range sizes and their responses to climate change in this area because no measurements have been previously conducted along the elevational gradient on both slopes in the Tianshan Mountains.

References

Aizen VB, Aizen EM, Melack JM, et al. (1997) Climatic and hydrologic changes in the Tien Shan, Central Asia. Journal of Climate 10: 1393-1404. https://doi.org/10.1175/1520-0442(1997)010<1393:cahcit>2.0.co;2

Barry RG (2008) Mountain Weather and Climate. Cambridge University Press, Cambridge, U. K.

Beniston M (2006) Mountain Weather and Climate: A general overview and a focus on climatic change in the Alps. Hydrobiologia 562(1): 3-16. https://doi.org/10.1007/s10750-005-1802-0

Blandford TR, Humes KS, Harshburger BJ, et al. (2008) Seasonal and synoptic variations in near-surface air temperature lapse rates in a mountainous basin. Journal of Applied Meteorology and Climatology 47(1): 249-261. https://doi.org/10.1175/2007jamc1565.1

Chae H, Lee H, Lee S, et al. (2012) Local variability in temperature, humidity and radiation in the Baekdu Daegan Mountain protected area of Korea. Journal of Mountain Science 9(5): 613-627. https://doi.org/10.1007/s11629-012-2347-0

Chan WP, Chen IC, Colwell RK, et al. (2016) Seasonal and daily climate variation have opposite effects on species elevational range size. Science 351(6280): 1437-1439. https://doi.org/10.1126/science.aab4119

Chen BX, Sun YF, Zhang HB, et al. (2018) Temperature change along elevation and its effect on the alpine timberline tree

growth in the southeast of the Tibetan Plateau. Advances in Climate Change Research 9(3): 185-191. https://doi.org/10.1016/j.accre.2018.05.001

Duane WJ, Pepin NC, Losleben ML, et al. (2008) General characteristics of temperature and humidity variability on Kilimanjaro, Tanzania. Arctic, Antarctic, and Alpine Research 40(2): 323-334. https://doi.org/10.1657/1523-0430(06-127)[duane]2.0.co;2

Deng H, Chen Y, Wang H, et al. (2015) Climate change with elevation and its potential impact on water resources in the Tianshan Mountains, Central Asia. Global and Planetary Change 135: 28-37. https://doi.org/10.1016/j.gloplacha.2015.09.015

Fang JY, Yoda K (1988) Climate and vegetation in China (I). Changes in the altitudinal lapse rate of temperature and distribution of sea level temperature. Ecological Research 3(1): 37-51. https://doi.org/10.1007/bf02348693

Gardner AS, Sharp MJ, Koerner RM, et al. (2009) Near-surface temperature lapse rates over arctic glaciers and their implications for temperature downscaling. Journal of Climate 22(16): 4281-4298. https://doi.org/10.1175/2009jcli2845.1

Guo L, Li L (2015) Variation of the proportion of precipitation occurring as snow in the Tian Shan Mountains, China: proportion of snowfall to precipitation. International Journal of Climatology 35(7): 1379-1393. https://doi.org/10.1002/joc.4063

Körner C (2004) Mountain biodiversity, its causes and function. Ambio, Special Report 13, 11-17.

Körner C (2007) The use of 'altitude' in ecological research. Trends in Ecology & Evolution 22(11): 569-574. https://doi.org/10.1016/j.tree.2007.09.006

Kirchner M, Faus-Kessler T, Jakobi G, et al. (2013) Altitudinal temperature lapse rates in an Alpine valley: trends and the influence of season and weather patterns. International Journal of Climatology 33(3): 539-555. https://doi.org/10.1002/joc.3444

Lundquist JD, Cayan DR (2007) Surface temperature patterns in complex terrain: Daily variations and long-term change in the central Sierra Nevada, California. Journal of Geophysical Research 112(D11): D11124. https://doi.org/10.1029/2006jd007561

Lundquist JD, Pepin NC, Rochford C (2008) Automated algorithm for mapping regions of cold-air pooling in complex terrain. Journal of Geophysical Research 113(D22): D22107. https://doi.org/10.1029/2008jd009879

Li X, Wang L, Chen D, et al. (2013) Near-surface air temperature lapse rates in the mainland China during 1962-2011. Journal of Geophysical Research: Atmospheres 118(14): 7505-7515. https://doi.org/10.1002/jgrd.50553

Li Y, Zeng Z, Zhao L, et al. (2015) Spatial patterns of climatological temperature lapse rate in mainland China: A multi-time scale investigation. Journal of Geophysical Research: Atmospheres 120(7): 2661-2675. https://doi.org/10.1002/2014jd022978

Liu B (2017). Vertical patterns in plant diversity and their relations with environmental factors on the southern slope of the Tianshan Mountains (middle section) in Xinjiang (China). Journal of Mountain Science 14(4): 742-757. https://doi.org/10.1007/s11629-016-4110-4

Liu SY, Yao XJ, Guo WQ, et al. (2015) The contemporary glaciers in china based on the second Chinese glacier inventory. Acta Geography Sinica 70(1): 3-16. (In Chinese)

Minder JR, Mote PW, Lundquist JD (2010) Surface temperature lapse rates over complex terrain: Lessons from the Cascade Mountains. Journal of Geophysical Research 115(D14). https://doi.org/10.1029/2009jd013493

Ngo-Duc T, Polcher J, Laval K (2005) A 53-year forcing data set for land surface models. Journal of Geophysical Research: Atmospheres 110(D6). https://doi.org/10.1029/2004jd005434

Pan Y, Yan S, Behling H, et al. (2013) Transport of airborne Picea schrenkiana pollen on the northern slope of Tianshan Mountains (Xinjiang, China) and its implication for paleoenvironmental reconstruction. Aerobiologia 29(2): 161-173. https://doi.org/10.1007/s10453-012-9270-2

Pepin NC (1994) The possible effects of climate change on the spatial and temporal variation of the altitudinal temperature gradient and the consequences for growth potential in the uplands of northern England. PhD thesis, Durham University.

Pepin NC, Bradley RS, Diaz HF, et al. (2015) Elevation-dependent warming in mountain regions of the world, Nature Climate Change 5(5): 424-430. https://doi.org/10.1038/nclimate2563

Pepin NC, Daly C, Lundquist J (2011) The influence of surface versus free-air decoupling on temperature trend patterns in the western United States. Journal of Geophysical Research 116(D10). https://doi.org/10.1029/2010jd014769

Petersen L, Pellicciotti F (2011) Spatial and temporal variability of air temperature on a melting glacier: Atmospheric controls, extrapolation methods and their effect on melt modeling, Juncal Norte Glacier, Chile: temperature variability over a glacier. Journal of Geophysical Research: Atmospheres 116(D23). https://doi.org/10.1029/2011jd015842

Prentice IC, Cramer W, Harrison SP, et al. (1992) Special Paper: A global biome model based on plant physiology and dominance, soil properties and climate. Journal of Biogeography 19(2): 117. https://doi.org/10.2307/2845499

Pagès M, Pepin NC, Miró JR (2017) Measurement and modelling of temperature cold pools in the Cerdanya valley (Pyrenees), Spain: Cold air pools in the Cerdanya valley (Pyrenees), Spain. Meteorological Applications 24(2): 290-302. https://doi.org/10.1002/met.1630

Rolland C (2003) Spatial and seasonal variations of air temperature lapse rates in alpine regions. Journal of Climate 16(7): 1032-1046. https://doi.org/10.1175/1520-0442(2003)016<1032:sasvoa>2.0.co;2

Sang W (2009) Plant diversity patterns and their relationships with soil and climatic elements along an altitudinal gradient in the middle Tianshan Mountain area, Xinjiang, China. Ecological Research 24(2): 303-314. https://doi.org/10.1007/s11284-008-0507-z

Schiemann R, Lüthi D, Vidale PL, et al. (2008) The precipitation climate of Central Asia—intercomparison of observational and numerical data sources in a remote semiarid region. International Journal of Climatology 28(3): 295-314. https://doi.org/10.1002/joc.1532

Shuttleworth WJ (2012) Terrestrial hydrometeorology. Hoboken, N.J: Wiley-Blackwell.

Shen YJ, Shen Y, Goetz J, et al. (2016) Spatial-temporal variation of near-surface temperature lapse rates over the Tianshan Mountains, central Asia: Variations of Lapse Rates. Journal of Geophysical Research: Atmospheres 121(23): 14,006-14,017. https://doi.org/10.1002/2016jd025711

Shen YJ, Shen Y, Fink M, et al. (2018) Trends and variability in streamflow and snowmelt runoff timing in the southern Tianshan Mountains. Journal of Hydrology 557: 173-181. https://doi.org/10.1016/j.jhydrol.2017.12.035

Sobel E, Chen J, Heermance R (2006) Late Oligocene–Early Miocene initiation of shortening in the Southwestern Chinese Tian Shan: Implications for Neogene shortening rate variations. Earth and Planetary Science Letters 247(1-2): 70-81. https://doi.org/10.1016/j.epsl.2006.03.048

Stone PH, Carlson JH (1979) Atmospheric lapse rate regimes and their parameterization. Journal of the Atmospheric Sciences 36(3): 415-423. https://doi.org/10.1175/1520-0469(1979)036<0415:alrrat>2.0.co;2

Tang Z, Fang J (2006) Temperature variation along the northern and southern slopes of Mt. Taibai, China. Agricultural and Forest Meteorology 139(3-4): 200-207. https://doi.org/10.1016/j.agrformet.2006.07.001

Wang X, Yang M, Liang X, et al. (2013) The dramatic climate warming in the Qaidam Basin, northeastern Tibetan Plateau, during 1961-2010. International Journal of Climatology 34(5): 1524-1537. https://doi.org/10.1002/joc.3781

Wang G, Zhao M, Kang M, et al. (2017) Diurnal and seasonal variation of the elevation gradient of air temperature in the northern flank of the western Qinling Mountain range, China. Journal of Mountain Science 14(1): 94-105. https://doi.org/10.1007/s11629-016-4107-z

Wason JW, Bevilacqua E, Dovciak M (2017) Climates on the move: Implications of climate warming for species distributions in mountains of the northeastern United States. Agricultural and Forest Meteorology 246: 272-280. https://doi.org/10.1016/j.agrformet.2017.05.019

Whittaker RJ, Willis KJ, Field R (2001) Scale and species richness: towards a general, hierarchical theory of species diversity. Journal of Biogeography 28(4): 453-470. https://doi.org/10.1046/j.1365-2699.2001.00563.x

Xu M, Kang S, Wu H, et al. (2018) Detection of spatio-temporal variability of air temperature and precipitation based on long-term meteorological station observations over Tianshan Mountains, Central Asia. Atmospheric Research 203: 141-163. https://doi.org/10.1016/j.atmosres.2017.12.007

Zhang C, Chen X, Shao H, et al. (2018) Evaluation and intercomparison of high-resolution satellite precipitation estimates—GPM, TRMM, and CMORPH, in the Tianshan Mountain area. Remote Sensing 10(10): 1543. https://doi.org/10.3390/rs10101543